Research article

Performance study on Ca-based sorbents for sequential CO_2 and SO_2 capture in a bubbling fluidised bed

Zhenghui Zhao [a], Kumar Patchigolla [b,*], Yinghai Wu [c], John Oakey [b], E.J. Anthony [b], Hongwei Chen [a]

[a] *Key Laboratory of Condition Monitoring and Control for Power Plant Equipment, North China Electric Power University, Baoding City, Hebei Province, People's Republic of China*
[b] *Centre for Thermal Energy Systems and Materials, Cranfield University, Cranfield, MK43 0AL, United Kingdom*
[c] *CanmetENERGY-Ottawa, Natural Resources Canada, 1 Haanel Dr., Ottawa, Ontario K1A 1M1, Canada*

ABSTRACT

High temperature CO_2 and SO_2 sequential capture in a bubbling fluidised bed was investigated using a natural limestone and synthetic composite pellets. Calcination was conducted under oxy-combustion conditions, while carbonation and sulphation occurred in an air-combustion atmosphere. The goal of sequential capture of CO_2/SO_2 is to desulphurise the flue gas first, followed by cyclic carbonation and calcination. Here, fresh sorbent is first used in the cyclic calcination/carbonation process and then the spent sorbent is sent for sulphation.

The pellet carrying capacity is 0.29 g CO_2/g sorbents for the first cycle, while that of natural limestone is about 0.45 g CO_2/g sorbents. The carrying capacity first fell and then finally plateaued around 0.10 and 0.12 g CO_2/g sorbents for limestone and pellets respectively. The SO_2 carrying capacity for limestone and pellets after 20 cycles of CO_2 capture was 0.17 and 0.22 g SO_2/g sorbents respectively. This indicates that the sorbent spent in CO_2 capture can be effectively reused for SO_2 removal. Abrasion was observed to be the main mode of attrition, but some agglomeration was also found with increasing number of cycles and this may be a concern in the use of Ca-based sorbent for CO_2 or SO_2 fluidised bed capture.

1. Introduction

The increased consumption of fossil fuels in power plants and incinerators has increased emission of air pollutants, including SO_2, which can cause acid rain, human respiratory irritation and diseases, and also serves as a precursor of extremely fine particulate matter [1]. CO_2 from the combustion of fossil fuels is a greenhouse gas, posing a global threat to the ecosystem. Over the last several decades, various technologies for reducing SO_2 emissions have been developed. Of these, the use of Ca-based sorbent to desulphurise flue gas is one of the most widely applied technologies [2]. Currently, Ca-based sorbent capture is receiving attention for CO_2 capture due to its economic advantages, namely high capacity and fast kinetics [3–5]. As both SO_2 and CO_2 can be captured by Ca-based sorbent, some attempts have been made to capture them simultaneously at high temperature [6,7]. However, generally the results from the cyclic co-capture of SO_2 and CO_2 in TGA and fluidised bed reactors confirm that SO_2 has a very negative effect on CO_2 capture [8,9]. The capacity of the sorbent to capture CO_2 decreases

rapidly when SO_2 is present and more rapidly as SO_2 concentration increases [10]. The pores on the sorbent surface are blocked by sulphation product more easily as the molar volume of $CaSO_4$ (46 cm³/mol) is higher than that of $CaCO_3$ (37 cm³/mol). More importantly, the unreacted CaO which is covered by sulphation product is prevented from reacting with CO_2 and permanently loses its carrying capacity because this product layer cannot be decomposed under calcination conditions. This adverse effect of SO_2 has been confirmed in several studies [11,12]. Manovic et al. used a Ca looping system with conditions suitable for both sulphation and carbonation [13]. Their results showed that sulphation and carbonation are competitive reactions when Ca-based sorbents are used for cleaning flue gas; and after a few cycles, the CO_2 capture capacity of the sorbent becomes negligible. The increase in the activity of a Ca-based sorbent for CO_2 capture typically leads to an increase in its activity toward SO_2. This means that any effort made for increasing sorbent performance for CO_2 capture is less effective if SO_2 is present [9,10]. These results suggest that ideally SO_2 must be avoided if the objective is CO_2 capture from flue gas, especially when more

---

efficient and more expensive sorbents are used in CO_2 capture systems. The use of a Ca-based sorbent to capture CO_2 and SO_2 sequentially can potentially solve this problem. The flue gas is first desulphurised and then decarbonated. In such a scheme the fresh Ca-based sorbent is first used to capture CO_2 cyclically and then the spent sorbent is used to capture SO_2 [14], as shown in the flow diagram in Fig. 1. The sulphation process can occur in a fluidised bed or in a separate reactor. For this work, a suitable Ca-based sorbent was developed to maintain an acceptable level of activity over a relatively high cycle number [here selected for a molar ratio of C/S in coal, which has 70 wt% C and 2 wt% S, resulting in a molar C/S ratio of 90]. Using this approach, a Ca-based sorbent employed to capture CO_2 can then be applied in a real power plant without producing any extra waste product [4,15].

Although the separate processes of CO_2 and SO_2 capture using Ca-based sorbent have been studied in both TGAs and fixed beds [16–18], fluidised bed systems are the most likely choice for a real system [19]. At this time various investigations have been conducted in pilot scale dual fluidised beds to test the effect of parameters, such as temperature, reaction time, and flow rate on sorbent carrying capacity [20–22]. Moreover, sorbent attrition is also an important concern because it helps determine fresh sorbent makeup flow rate. In the present study, a bench scale bubbling fluidised bed was used to perform calcination/carbonation cycles and a final sulphation step with different temperatures and gas composition. This experimental setup has the advantage that samples can be withdrawn from the reactor to characterize them in terms of their physical and chemical properties.

To simulate a realistic environment, the gas composition for calcination was chosen based on the calculation of the likely composition for oxy-combustion of Daw Mill coal from UK, which has been studied extensively [23]. The steam that is present in flue gas was reproduced by injecting water with a small water metering pump. Borgwardt et al. reported that porosity reduction and sorbent sintering were accelerated by steam [24], while other researchers have demonstrated a significant positive influence of steam on sulphation and carbonation [25–27]. In addition, however, steam generates cracks on the surface of natural sorbent and intensifies solid attrition [19,28,29]. A significant increase in the attrition of limestone was observed after the reactivation of sorbent by hydration in a bench-scale fluidised bed [25]. In the present paper, the effect of steam on the natural limestone and pellets synthesized from lime and calcium alumina cement was also examined.

Most research [16–18] focuses on sorbent conversion and microstructure, and often the sorbent macro morphology is not investigated. One of the immediate observations was that powdered fresh limestone formed clumps after a few CO_2 looping cycles or even after the first calcination in a TGA or fixed bed. Although these clumps are easily destroyed by shaking or stirring in a small reactor, whether they would influence the fluidisation effect in a full-scale system is uncertain, especially in the presence of steam in the flue gas. In the present work, considerable attention was paid to whether or not the solid

agglomeration phenomenon affects the fluidisation effect. This phenomenon can be easily overlooked in pilot scale or even larger pilot scale fluidised beds because the run time is usually short and such phenomena can be alleviated by varying gas flow rate [30], but this may influence the circulating rate of solids or cause defluidisation over long timescales. The current work explores an economical approach to capture SO_2 and CO_2 sequentially using an abundant and inexpensive natural sorbent. The results are expected to provide a reference for large scale application of Ca-based sorbent with CO_2 and SO_2 capture in fluidised bed.

2. Experimental methodology

2.1. Samples

Longcliffe limestone from the UK and a Ca-based pellet sorbent were used in the experiments. Longcliffe limestone is one of most widely used industrial limestones in the UK, as it is soft and easily ground to fine powder. It can be regarded as an ideal SO_2/CO_2 sorbent due to its high $CaCO_3$ content (over 98.25%). The limestone was ground and sieved on an electric vibrating screen. Fine particles have large surface area which typically produces better sorbent performance in SO_2/CO_2 capture, but too fine particles are more likely to be elutriated from the reactor. A compromise of particle size of 125–250 μm was selected. To verify the SO_2/CO_2 capacity and as a comparison research, Ca-based pellets which were made of limestone and calcium aluminate cement with a mass ratio of 9:1, based on our previous study [31], were also used in this work. Cadomin limestone (Canada), particle size 0.25–1.4 mm, was used for the pellets. Commercial calcium aluminate cement, containing ~71% Al_2O_3, ~28% CaO, and ~1% impurities (Na_2O, SiO_2, Fe_2O_3, MgO), produced by Almatis Inc., was used as binder. The composition of the pellets and the pelletisation process have been described elsewhere [32]. The obtained pellets size was 125–875 μm. The macroscopic features of these materials are shown in Fig. 2.

2.2. Experimental apparatus and procedures

The calcination and carbonation multicycles, as well as the sulphation step, were conducted in a fluidised bed reactor, as shown in Fig. 3. The major components of the FBC system are an outer tube furnace with a height of 1180 mm and an internal diameter of 37 mm, and an inner quartz reactor with a height of 550 mm and an internal diameter of 32 mm. Samples (10–60 g) were loaded into the reactor and then placed into the tube furnace. The simulated flue gas carrying the steam from the water pump into the tube furnace was preheated in the lower part before entering the reactor through a distributor in the bottom of the reactor. The hot flue gas passed through a filter, and then a part of the flue gas was diverted to the gas analyzer. An electrical heater surrounding the outer tube was used to keep the temperature above the acid dew point to prevent condensation. The composition of the simulated gas was controlled by a set of highly accurate mass flow controllers (MFCs). A computer was used in this system to record the data from gas analyzer and thermocouples, as well as to control the MFCs.

To keep solids well fluidised, a relatively high gas velocity of 0.22 m/s was selected ($U/U_{mf} \approx 11$, $U/U_t \approx 0.035$ for limestone). Before undergoing sulphation, the samples experienced different number of CO_2 capture looping cycles to test their performance. To obtain a high-concentration CO_2 stream and provide heat for sorbent regeneration, calcination was performed in a simulated oxy-combustion environment (i.e., 80% CO_2 + 16% H_2O + 3% O_2 + 1% N_2) at 950 °C for 20 min. In previous studies, the carbonation displayed a fast reaction at about 700 °C and the reaction changes from dynamic control stage to diffusion control stage in about 2 or 3 min. The diffusion-controlled reaction lasted for 10 to 20 min [33]. The optimized sulphation temperature is 850–900 °C. Here, the sulphation process was slower than carbonation, and even at 90 min the sulphation curve was still increasing slightly. In
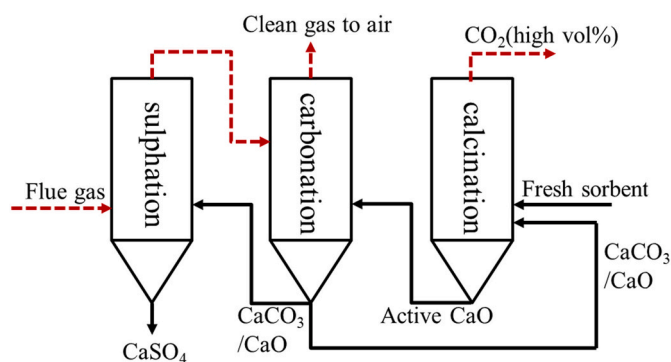

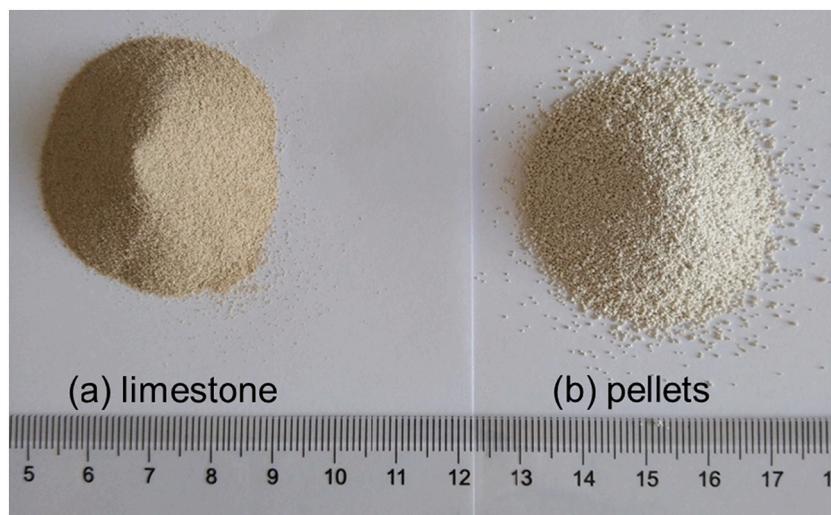**Fig. 1.** The flow diagram for Ca-based sorbent to capture CO_2 and SO_2 sequentially.

Fig. 2. The image of fresh limestone and pellets.

size distribution (PSD) was also examined by laser particle size analyzer.

2.3. Analysis

The sorbent carrying capacity was calculated by integration of the difference between inlet and outlet gas concentrations recorded online. The formula used for the calculation is as follows:

$$X = \frac{M_{\text{gas}}}{V * m} \int_0^t q * \frac{C^0 - C^t}{1 - C^t} \, \mathrm{d}(t) \tag{1}$$

where q is the fluidising gas flow rate, L/s; V is gas molar volume at standard conditions, which is 22.4 L/mol; m is the initial calcined solid mass, g; M_{gas} is CO_2 or SO_2 molar mass, g/mol; C^0 is the CO_2 or SO_2 percentage (by volume) of gas entering the reactor, C^t is the CO_2 or SO_2 percentage (by volume) of gas exiting the reactor; and X is the sorbent carrying capacity after time t, g CO_2(SO_2)/ g calcined sorbent.

3. Results and discussion

3.1. Sorbent conversions

Fig. 4 shows the CO_2 capture profiles, obtained from the fluidised bed and without the influence of SO_2. The Longcliffe limestone and the
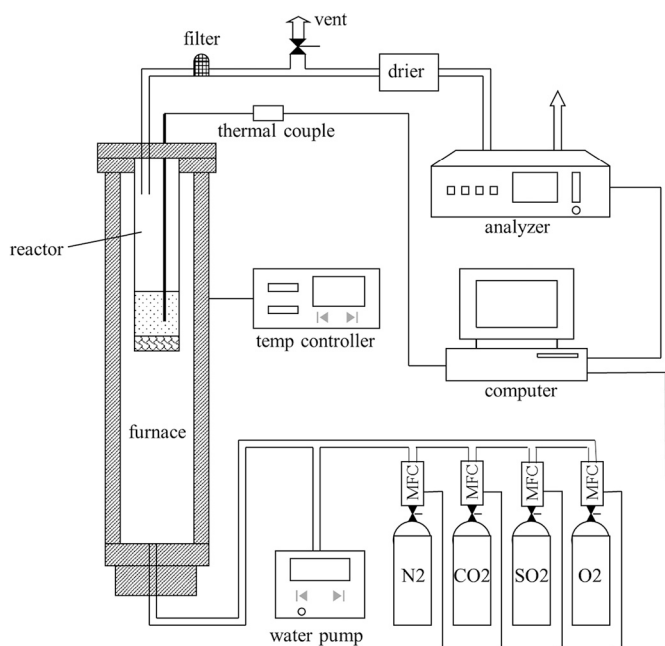

Fig. 3. Scheme of the experimental system.

order to obtain a full carbonation/sulphation conversion, carbonation was performed in a simulated air-combustion environment but without the presence of SO_2 (i.e., 15% CO_2 + 6% H_2O + 3% O_2 + 76% N_2) at 700 °C for 20 min. Sulphation was then conducted in a simulated air-combustion environment (i.e., 15% CO_2 + 6% H_2O + 3% O_2 + 75.88% N_2 + 0.12% SO_2) at 900 °C for 90 min. The transition between carbonation and calcination was realized by changing the temperature and atmosphere. When calcination finished, the temperature was decreased from 950 to 700 °C and at the same time the gas stream was changed to simulate a carbonation atmosphere. When carbonation was finished, the temperature was increased and the gas changed into a calcination atmosphere. The gas compositions were calculated based on the composition of Daw Mill coal. When the experiment was completed, the reactor was removed and the samples were photographed with a digital camera. The microstructure of samples was analyzed by scanning electron microscope (SEM). Brunauer-Emmett-Teller (BET) surface area and pore volume measurements were performed by using nitrogen adsorption and desorption isotherms at liquid N_2 temperature. Particle
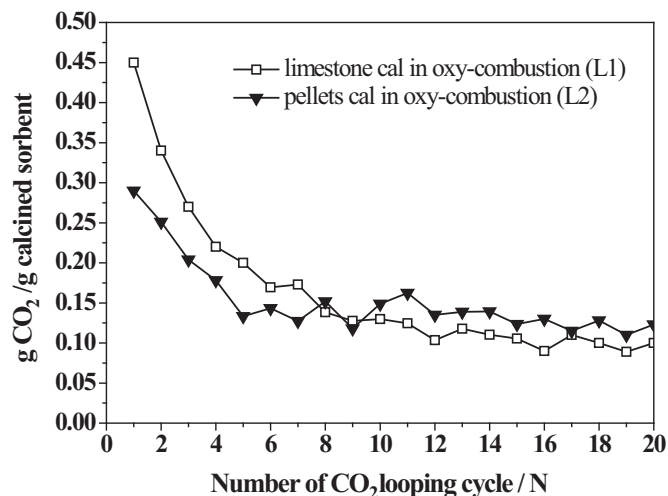

Fig. 4. CO_2 carrying capacity of sorbents versus looping cycle in fluidised bed.

pellets were calcined before the performance tests. Their mass losses of calcination were 43.1% and 31.3%, respectively, at 950 °C under N_2 atmosphere for 2 h. The CO_2 carrying capacity was about 0.45 g CO_2/g sorbent for fresh calcined limestone and decreased as the cycle number increased and remained at 0.10 g CO_2/g sorbent after twenty cycles, with a decrease of 78%. The carrying capacity for fresh pellets was 0.29 g CO_2/g sorbent, lower than that for limestone due to the presence of less active components (in particular the calcium aluminate cement binder which does not react with CO_2). After 10 cycles, the carrying capacity for pellets exceeded that for limestone and maintained a capacity of 0.12 g CO_2/g sorbent up to 20th cycle, representing a decrease of 59%, indicating that pellets have better long-term cyclic activity than natural limestone.

A significant phenomenon observed in the experiment is that the solids adhere together with increasing number of cycles, which is easily overlooked in TGA experiments. The agglomerated particles cannot be easily fluidised and finally cause defluidisation despite the vigorous fluidisation conditions. The fluidisation condition has some effect on the solid carrying capacity. During the first few cycles (five cycles), sorbent performance reduced steadily, which means sorbent performance decreased due to sorbent characteristics and was not influenced by fluidisation conditions, whereas after five cycles, the solids started to agglomerate, causing fluctuation in the sorbent performance.

To verify whether the carrying capacity calculated from gas composition analysis is in line with that calculated from solid weight analysis, the solids were collected from the reactor at given intervals and the weight was measured. After measurement, the agglomerated solids were broken up and then used again in the reactor where they exhibited nearly the same or even better carrying capacity in the next cycle indicating that defluidisation is a major potential problem for a bubbling bed system.

TGA results have shown that after multiple calcination/carbonation cycles, the spent Ca-based sorbent is still active for SO_2 retention [14]. Here, the SO_2 capture capacity of Ca-based sorbent obtained after different numbers of cycles was tested in a fluidised bed under simulated flue gas atmosphere. The results are presented in Fig. 5. The SO_2 capture capacity decreased with increasing number of CO_2 looping cycles for both limestone and pellets. The SO_2 capture capacities for fresh calcined limestone and pellets are 0.35 and 0.47 g SO_2/g sorbent, respectively. After 20 CO_2 capture cycles, the SO_2 carrying capacities for limestone and pellets are 0.17 and 0.22 g SO_2/g sorbent, indicating that the sorbent spent in CO_2 capture can be reused in SO_2 retention. An interesting result is that the pellets have considerably better performance for SO_2

capture than does limestone, although pellets have less active CaO available due to the presence of a binder. However, the pellets did not have significantly better CO_2 carrying capacity than limestone, as showed in Fig. 4, indicating the binder appears to benefit SO_2 capture but not CO_2 capture for these tests. The possible reason for the improved SO_2 capture performance for pellets may be that some metal cations like Na^+ were introduced into the pellets as well as lattice imperfections formed at high temperature condition when the cement was used as a binder [34]. Besides kinetic and gas diffusion control, solid ion diffusion plays a significant role in sulphation but not in the carbonation process [35]. Solid ions diffuse by means of these lattice imperfections. The more vacancy defects there are, the faster the ion transfer and the reaction [34].

3.2. Sorbent morphology

Table 1 shows the BET surface area, pore volume, and average pore diameter of the samples from different runs. When limestone was calcined for the first time, its surface area and pore volume drastically increased from 0.3389 m^2/g to 9.9470 m^2/g and from 0.0008 cm^3/g to 0.0354 cm^3/g, respectively. After the 15th calcination, as expected, both surface area and pore volume decreased, while the pore diameter increased due to sintering. After carbonation or sulphation, the pores were blocked by the product, except for those with diameters larger than twice that of the product layer. Thus, the average diameter of the remaining unblocked pores considerably increased. The original pellets were mainly composed of $Ca(OH)_2$ and had considerably larger surface area (22.49 m^2/g) and pore volume (0.09 cm^3/g) when compared with the original limestone or calcined limestone. The surface area and pore volume of pellets exhibited impressive values of 7.09 m^2/g and 0.03 cm^3/g, respectively, even after 20 calcinations, which is desired, as high surface area and pore volume are necessary for a better cyclic activity.

Fig. 6 shows the SEM images for limestone and pellets at different stages in the cyclic CO_2 capture and final sulphation step. It can be clearly seen that cracks formed on the surface of the limestone as the cycle number increased, but not for the pellets. After the 5th calcination, as shown in Fig. 6 (a), only a few wide and long cracks were formed on the surface of the calcine, but abundant small cracks were also found. After the 15th calcination, the small cracks enlarged, thereby dividing the particle surface into many small distinct areas, as shown in Fig. 6 (b). The formation of cracks can be attributed to the presence of steam in the calcination stage and in the carbonation atmosphere. A similar phenomenon was reported previously when steam was introduced into the
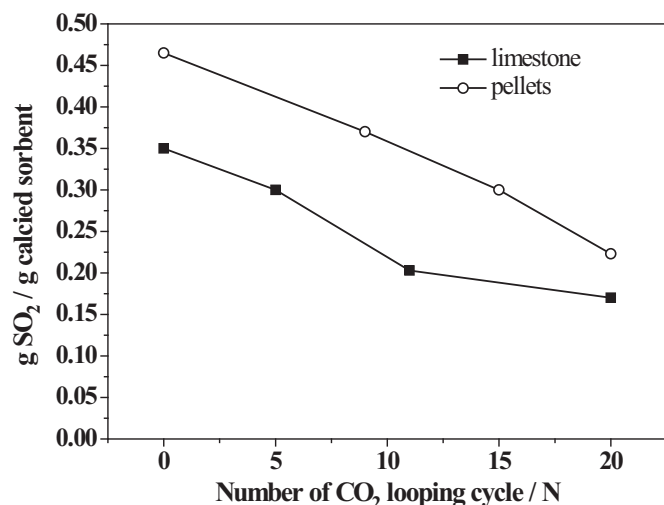
Fig. 5. SO_2 carrying capacity of sorbents after different CO_2 looping cycles in fluidised bed.

Table 1
BET pore surface areas and BJH cumulative pore volumes of samples.

Sample	BET surface area (m^2/g)	Cumulative volume of pores (1.7–300 nm) (cm^3/g)	Average pore diameter (4 V/A) (nm)
Original limestone	0.34	0.001	14.03
Limestone 1 cal	9.95	0.04	14.66
Limestone 15 cal	3.89	0.02	18.21
Limestone 20car	0.39	0.002	25.51
Limestone 20 cal-sul	3.37	0.0004	24.19
Original pellets	22.49	0.09	14.66
Pellets 20 cal	7.09	0.03	13.32
Pellets 20 cal-sul	1.42	0.004	11.99

Note: "limestone/pellets number cal" means "number" of calcinations.
"limestone/pellets number car" means "number" of carbonations.
"limestone/pellets number cal-sul" means "number" of calcinations and then being sulphated.
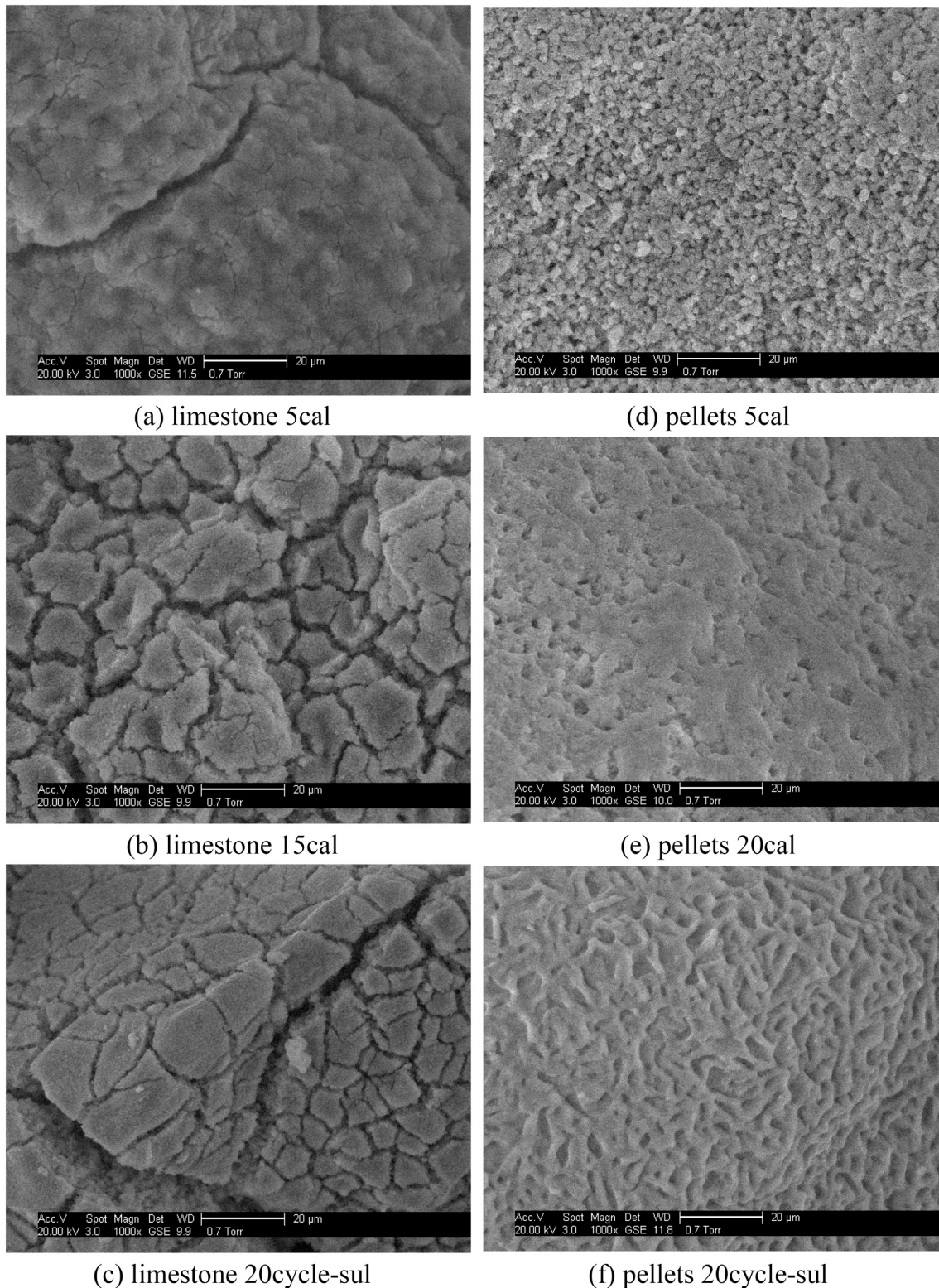
(a) limestone 5cal

(d) pellets 5cal

(b) limestone 15cal

(e) pellets 20cal

(c) limestone 20cycle-sul

(f) pellets 20cycle-sul

Fig. 6. SEM images of particle surface morphologies for limestone and pellet after different runs.

flue gas [36,37]. Cracks increase the solid–gas interface and provide extra space for product growth while providing the path for gas to penetrate into the interior of the particles, thereby benefiting CO_2 or SO_2 capture. On the other hand, the cracks also increase the fragility of the particle and cause intensified attrition in a FBC system, thus explaining why sorbents experience severe attrition after hydration [19]. Therefore, although the introduction of steam into the CO_2 and SO_2 capture process improves the activity of the sorbent, it also accelerates attrition. After sulphation, as shown in Fig. 6 (c), most of the cracks narrowed but were still visible, indicating that the width of cracks was considerably larger than twice that of the sulphation product thickness. Under the same condition, the surface morphology of pellets was totally transformed. Comparison of Figs. 6 (d) and (e) showed that the pellet surface smoothed with increasing number of cycles, and no cracks were formed.

This finding indicates that the aluminate cement binder increased the strength of the pellets, which is important for mitigating attrition. After sulphation, as shown in Fig. 6 (f), more pronounced macropores were formed. However, the positive contribution of these macropores to surface area and sorbent conversion is offset because once the $CaSO_4$ product is formed on the surface of particles, the reaction is limited by the diffusion rate of gas into the particles. This also explains why sorbent activity decreased more quickly in CO_2 capture cycles in the presence of SO_2: not only because some sorbent is irreversibly converted into $CaSO_4$, but also because the $CaSO_4$ shell impeded the contact of CO_2 with the interior CaO content [38].

3.3. Particle attrition and agglomeration

Under fluidised bed conditions, sorbents are subjected to mechanical stress, such as impact and shear, and thermal stress, which increases the severity of attrition. Different environments in the carbonator and calciner resulted in different attrition behavior. Fragmentation and abrasion are the two modes of particle attrition [39]; the former created new particles with a size of the same order of magnitude as the original ones, while the latter generated very fine particles that are scraped off from the surface of the original particles. In this bench scale fluidised bed, attrition tests were also conducted during CO_2 capture cycles. The particle-size distributions (PSD) of limestone and pellets are shown in Fig. 7. The mass distribution shifted from large to small size after 10 cycles in both cases. The average sizes for the original limestone and sorbent after 10 calcinations were 198 and 187 μm, respectively. The pellets employed here are considerably larger than the limestone, and therefore the attrition property is different. Large particles have more inertia and are consequently associated with more energetic collisions. As expected, large particles suffered more severe attrition than small ones. After 10 calcinations, the portion of particles with a size larger than 780 μm decreased substantially. The average size of pellets decreased from 579 μm to 543 μm. Only one peak was observed in each distribution, thereby suggesting that fragmentation did not happen randomly during CO_2 capture cycles [40,41], and abrasion appears to be the main mode of attrition. Here, some extremely fine particles generated by abrasion were carried out of the reactor by the fluidising gas. This unavoidable elutriation may result in the slightly higher measured value of cycled particle size compared with the real value [42].

Apart from the attrition phenomenon, agglomeration was also observed in all tests. The particles agglomerated when the cohesive force between the particles was stronger than the gravitational and drag forces. The cohesive force may arise due to the different types of interactions: van der Waals, electrostatic, capillary, viscous, sintering, adhesive, and chemical reaction. Pictures of the particles in the reactor tube after various numbers of cycles are shown in Fig. 8. After fresh limestone was calcined for the first time, most of the solids were still powdery, with only a few agglomerates (Fig. 8 a). After nine full CO_2 capture cycles and by the end of the 10th calcination, the solids were no longer powdery, especially near the wall of the reactor (as shown in Fig. 8 b). This result is a major concern if the use of limestone to capture CO_2 is applied to a full scale FBC system. A lower sorbent conversion was expected because the agglomerates hinder gas–solid contact. Interestingly, the bonding strength between solids was not as strong as expected, and the agglomeration is clearly different from that reported in literature for biomass combustion in FBC [43,44]. The cycle number and the sulphation products (namely anhydrite) aggravated solid agglomeration as shown in Fig. 8 c. Modified Ca-based pellets, with considerably larger particle size than limestone, demonstrated considerable agglomeration, as seen in Fig. 8d, e, f. The larger size particles had bigger voids, and smaller surface area contact with each other; and thus, a stronger bonding strength was required to agglomerate them. Meanwhile, more energetic collisions between large particles decreased agglomeration [45]. After 14 full cycles (Fig. 8e), most of the agglomerates were found at the bottom of the reactor, with only a few solids agglomerates near the wall; however, by the end of the 20th calcination, more agglomerated solids had accumulated near the wall. Once the solids started to agglomerate, the flow of fluidised gas became uneven, and more solids were likely to agglomerate in the dead zones. These results demonstrate that the agglomeration progressively built up at the bottom of the bed and near the wall, eventually leading to total bed defluidisation.

This phenomenon should not be overlooked because a continuous examination of solid conditions in the reactor is challenging, especially in pilot-scale or full-scale fluidised beds. In this study, as a transparent quartz tube reactor was used, the sorbent could be observed visually and pictures could be taken with a digital camera at the end of experiment. Increasing the turbulence in the fluidised bed by increasing the gas velocity may have alleviated particle agglomeration, but the loss of fine particles also increased. In fact, the possibility of agglomeration was only postponed rather than eliminated, by increasing gas velocity in our tests. A relatively high velocity of 0.22 m/s (U/$U_{mf} \approx 11$, U/$U_t \approx 0.035$ for limestone) was selected as a compromise between particle agglomeration and particle loss. Here, the diameter of the quartz reactor was 32 mm, which could be one factor that aggravated the severe agglomeration. The electrostatic force caused by friction of particles with the reactor wall allowed sticking of particles on the wall, thereby explaining why more solids agglomerated near the wall than in the center of the reactor [46]. Jia et al. also mentioned that limestones exhibited clear agglomeration behavior in the laboratory fluidised bed for a small-sized reactor [47]. This finding might be attributed to the fact that lime or limestone becomes relatively soft and plastic at high temperature, thereby providing the possibility for sticking together of the particles. Intermolecular and electrostatic forces caused by the friction between particles aid the agglomeration of particles. In addition, the steam that exists in the reactant gas may also promote agglomeration.
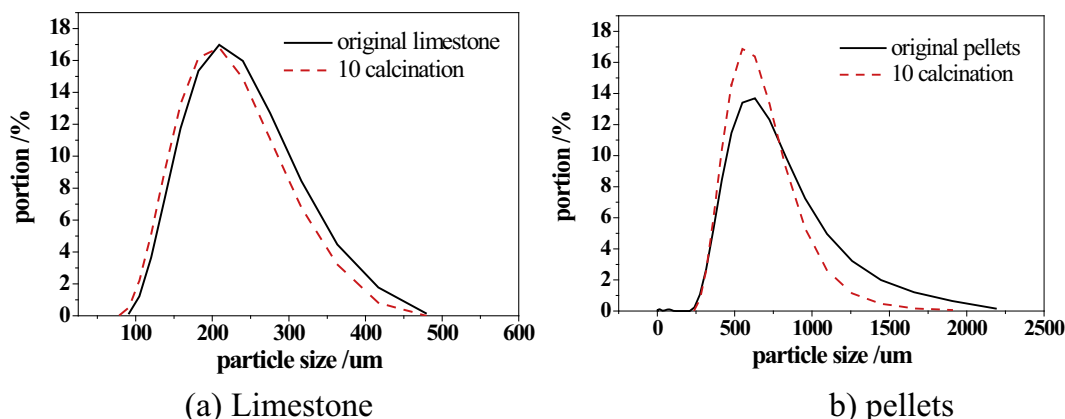

(a) Limestone   b) pellets

Fig. 7. Particle size distribution for limestone and pellets.

a) Limestone, 1 cal   b) Limestone, 10 cal   c) Limestone, 20 cal then sul

d) Pellets, 1 cal   e) pellets, 14 car   f) pellets, 20 cal
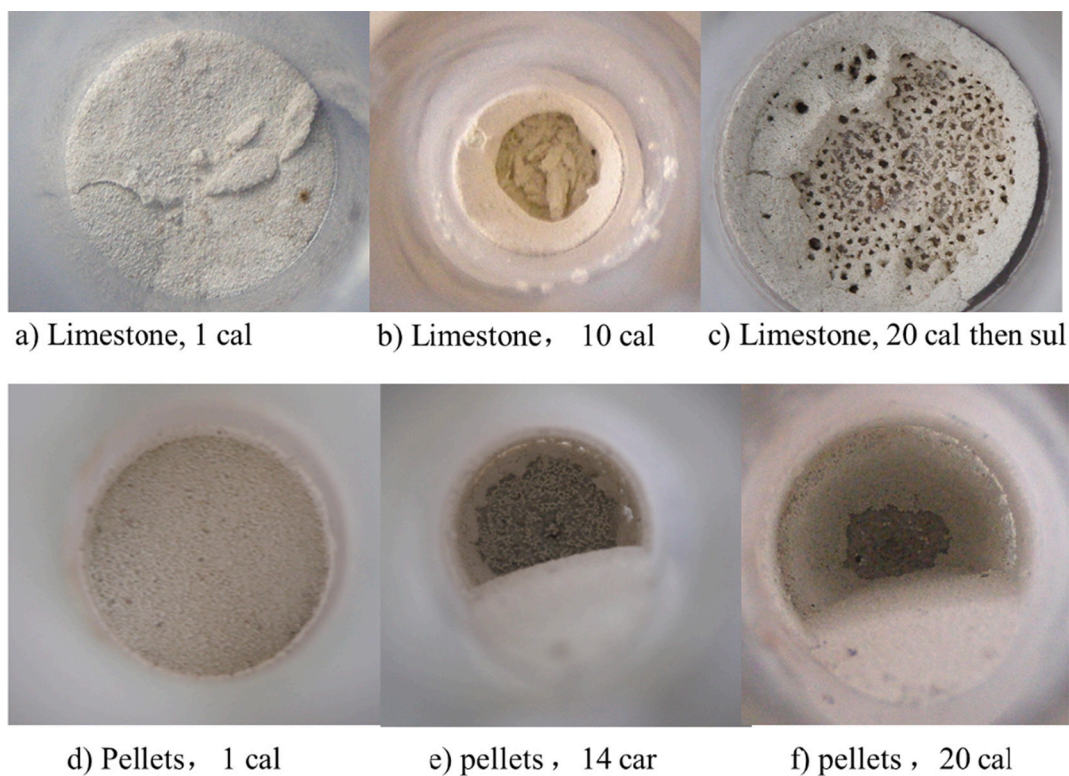
Fig. 8. Agglomeration of particles in fluidised bed.

4. Conclusions

The performance of the Ca-based sorbents (limestone and pellets) for sequential CO_2 and SO_2 capture was tested in a bubbling fluidised bed. The pellets showed better performance in long-term CO_2 capture looping and SO_2 retention due to larger surface area, although they had slightly lower CO_2 carrying capacity than limestone in the first few cycles due to the nonreactive component of calcium aluminate cement ($CaAl_2O_4$) binder. The SO_2 carrying capacities for limestone and pellets which had experienced 20 CO_2 capture cycles were 0.17 and 0.22 (g SO_2/g calcined sorbents), respectively, indicating that the sorbent spent in CO_2 capture can be reused in SO_2 retention.

The large particles endured more severe abrasion than the small ones, causing a shift in particle size distribution from large to small. The steam was believed to benefit sorbent conversion, but also intensified sorbent attrition by creating cracks on the surface of the limestone. No cracks but rather a smoother surface was observed for the pellets due to the presence of a binder.

Agglomeration was found to be a concern in the use of Ca-based sorbent to capture CO_2 or SO_2 in the fluidised bed system. The sorbents became less powdery after a few cycles, affecting the fluidisation and even creating defluidisation regions. More investigations are necessary to study agglomeration in-situ especially in a large-scale fluidised bed and to analyze the reasons before developing possible countermeasures.

Declaration of Competing Interest

The authors declare that they have no known competing financial interests or personal relationships that could have appeared to influence the work reported in this paper.

References

[1] G. Cheng, C. Zhang, Desulfurization and denitrification technologies of coal-fired flue gas, Pol. J. Environ. Stud. 27 (2018) 481–489.

[2] J. Cheng, J. Zhou, J. Liu, Z. Zhou, Z. Huang, X. Cao, X. Zhao, K. Cen, Sulfur removal at high temperature during coal combustion in furnaces: a review, Prog. Energy Combust. Sci. 29 (5) (2003) 381–405.

[3] M. Haaf, R. Anantharaman, S. Roussanaly, J. Strohle, B. Epple, CO_2 capture from waste-to-energy plants: Techno-economic assessment of novel integration concepts of calcium looping technology, Resources, Conserv. Recycl. 162 (2020), 104973.

[4] Y. Hu, H. Lu, W. Liu, Y. Yang, H. Li, Incorporation of CaO into inert supports for enhanced CO_2 capture: a review, Chem. Eng. J. 396 (2020) 125253.

[5] Y. Hu, W. Liu, Y. Peng, Y. Yang, J. Sun, H. Chen, Z. Zhou, M. Xu, One-step synthesis of highly efficient CaO-based CO_2 sorbent pellets via gel-casting technique, Fuel Process. Technol. 160 (2017) 70–77.

[6] H. Ryu, J.R. Grace, C.J. Lim, Simultaneous CO_2/SO_2 capture characteristics of three limestones in a fluidized-bed reactor, Energy Fuel 20 (4) (2006) 1621–1628.

[7] C. Wang, L. Jia, Y. Tan, Simultaneous carbonation and sulfation of CaO in oxy-fuel CFB combustion, Chem. Eng. Technol. 34 (10, 2011) 1685–1690.

[8] P. Sun, J.R. Grace, C.J. Lim, E.J. Anthony, Removal of CO_2 by calcium-based sorbents in the presence of SO_2, Energy Fuel 21 (1) (2007) 163–170.

[9] H. Lu, P.G. Smirniotis, Calcium oxide doped sorbents for CO_2 uptake in the presence of SO_2 at high temperatures, Ind. Eng. Chem. Res. 48 (11, 2009) 5454–5459.

[10] C. Luo, Y. Zheng, J. Guo, B. Feng, Effect of sulfation on CO_2 capture of CaO-based sorbents during calcium looping cycle, Fuel 127 (2) (2014) 124–130.

[11] A. Coppola, F. Montagnaro, P. Salatino, F. Scala, Fluidised bed calcium looping: the effect of SO_2 on sorbent attrition and CO_2 capture capacity, Chem. Eng. J. 207–208 (10, 2012) 445–449.

[12] S. Chen, C. Qin, T. Deng, J. Yin, J. Ran, Particle-scale modeling of the simultaneous carbonation and sulfation incalcium looping for CO_2 capture, Sep. Purif. Technol. 252 (2020) 117439.

[13] V. Manovic, E.J. Anthony, Competition of sulphation and carbonation reactions during looping cycles for CO_2 capture by CaO-based sorbents, J. Phys. Chem. A 114 (11, 2010) 3997–4002.

[14] H. Chen, Z. Zhao, X. Huang, K. Patchigolla, A. Cotton, J. Oakey, Novel optimized process for utilization of CaO-based sorbent for capturing CO_2 and SO_2 sequentially, Energy Fuel 26 (9) (2012) 5596–5603.

[15] S. Yasipourtehrani, S. Tian, V. Strezov, T. Kan, T. Evans, Development of robust CaO-based sorbents from blast furnace slag for calcium looping CO_2 capture, Chem. Eng. J. 387 (2020) 124140.

[16] V. Manovic, E.J. Anthony, Steam Reactivation of spent CaO-based sorbent for multiple CO_2 capture cycles, Environ. Sci. Technol. 41 (2007) 1420–1425.

[17] S.A. Salaudeen, B. Acharya, A. Dutta, CaO-based CO_2 sorbents: a review on screening, enhancement, cyclic stability, regeneration and kinetics modelling, J. CO2 Util. 23 (2018) 179–199.

[18] Y. Mathieu, L. Tzanis, M. Soulard, et al., Adsorption of SO_X by oxide materials: a review, Fuel Process. Technol. 114 (2013) 81–100.

[19] V. Manovic, D. Lu, E.J. Anthony, Steam hydration of sorbents from a dual fluidised bed CO_2 looping cycle reactor, Fuel 87 (2008) 3344–3352.

[20] P.T. Clough, G. Greco, M. Erans, A. Coppola, F. Montagnaro, E.J. Anthony, The extent of sorbent attrition and degradation of ethanol-treated CaO sorbents for CO_2 capture within a fluidised bed reactor, Fuel Process. Technol. 171 (2018) 198–204.

[21] A. Charitos, C. Hawthorne, A.R. Bidwe, S. Sivalingam, A. Schuster, H. Spliethoff, G. Scheffknecht, Parametric investigation of the calcium looping process for CO_2 capture in a 10kWth dual fluidised bed, Int. J. Greenh. Gas Con. 4 (5) (2010) 776–784.

[22] M. Abreu, P. Teixeira, R.M. Filipe, L. Domingues, C.I.C. Pinheiro, H.A. Matos, Modeling the deactivation of CaO-based sorbents during multiple Ca-looping cycles for CO_2 post-combustion capture, Comput. Chem. Eng. 134 (2020) 106679.

[23] N. Jurado, H.G. Darabkhani, E.J. Anthony, J.E. Oakey, Oxy-fuel combustion for carbon capture and sequestration (CCS) from a coal/biomass power plant: experimental and simulation studies, Prog. Clean Energy 2 (2015) 177–192.

[24] R.H. Borgwardt, Calcium oxide sintering in atmospheres containing water and carbon dioxide, Ind. Eng. Chem. Res. 28 (4, 1989) 493–500.

[25] V. Manovic, E.J. Anthony, Carbonation of CaO-Based sorbents enhanced by steam addition, Ind. Eng. Chem. Res. 49 (19, 2010) 9105–9110.

[26] M. Kavosh, K. Patchigolla, E.J. Anthony, J.E. Oakey, Carbonation performance of lime for cyclic CO_2 capture following limestone calcination in steam/CO_2 atmosphere, Appl. Energy 131 (2014) 499–507.

[27] P. Yang, Z. Sun, L. Duan, H. Tang, Mechanism of steam-declined sulfation and steam-enhanced carbonation by DFT calculations, Greenh. Gases Sci. Technol. 10 (2) (2020) 472–483.

[28] H. Chen, Z. Zhao, X. Huang, X. Huang, Sequential SO_2/CO_2 capture using CaO-based sorbents reactivated by steam, CIESC J. 63 (8) (2012) 2567–2575.

[29] J. Blamey, N.P.M. Paterson, D.R. Dugwell, P.S. Fennell, Mechanism of particle breakage during reactivation of CaO-based sorbents for CO_2 capture, Energy Fuel 24 (8) (2010) 4605–4616.

[30] J. Hilz, M. Helbig, M. Haaf, A. Daikeler, J. Strohle, B. Epple, Long-term pilot testing of the carbonate looping process in 1 MW_{th} scale, Fuel 210 (2017) 892–899.

[31] V. Manovic, E.J. Anthony, Screening of binders for pelletisation of CaO-based sorbents for CO_2 capture, Energy Fuel 23 (2009) 4797–4804.

[32] Yinghai Wu, Vasilije Manovic, Ian He, Edward J. Anthony, Modified lime-based pellet sorbents for high-temperature CO_2 capture: Reactivity and attrition behavior, Fuel 96 (2012) 454–461.

[33] H. Chen, Z. Zhao, W. Wang, Factors influencing simultaneous CO_2/SO_2 capture by Ca-based sorbent and evolution of the limestone surface structure, J. Chin. Soc. Power Eng. 33 (3) (2013) 210–217.

[34] C. Wang, X. Shen, The investigation on the sulfation mechanisms of Ca-based sorbent modified by Na_2CO_3, J. Eng. Thermophys. 23 (5) (2002) 641–644.

[35] W.L. Duo, K. Laursen, J. Lim, Crystallization and fracture: product layer diffusion in sulfation of calcined limestone, Ind. Eng. Chem. Res. 43 (18, 2004) 5653–5662.

[36] V. Manovic, E.J. Anthony, Sequential SO_2/CO_2 capture enhanced by steam reactivation of a CaO-based sorbent, Fuel 87 (8–9) (2008) 1564–1573.

[37] S. Rahiala, J. Ritvanen, T. Hyppänen, T. Pikkarainen, Bench-scale and modelling study of the effect of H_2O on sulphur capture by limestone in conditions of fluidized-bed air combustion and oxycombustion, Fuel 196 (2017) 233–240.

[38] C. Luo, Y. Zheng, J. Yin, C. Qin, N. Ding, C. Zheng, B. Feng, Effect of sulfation during oxy-fuel calcination stage in calcium looping on CO_2 capture performance of CaO-based sorbents, Energy Fuel 27 (2) (2013) 1008–1014.

[39] S. Maurer, S.R. Durán, M. Künstle, S.M.A. Biollaz, Influence of interparticle forces on attrition and elutriation in bubbling fluidised beds, Powder Technol. 291 (2016) 473–486.

[40] G. Xiao, J.R. Grace, C.J. Lim, Attrition characteristics and mechanisms for limestone particles in an air-jet apparatus, Powder Technol. 207 (1–3) (2011) 183–191.

[41] Z. Chen, J.R. Grace, C.J. Lim, Limestone particle attrition and size distribution in a small circulating fluidized bed, Fuel 87 (7) (2008) 1360–1371.

[42] F.N. Ridha, D.Y. Lu, R.T. Symonds, S. Champagne, Attrition of CaO-based pellets in a 0.1 MW dual fluidized bed pilot plant for post-combustion CO_2 capture, Powder Technol. 291 (2016) 60–65.

[43] A. Grimm, N. Skoglund, D. Boström, M. Öhman, Bed agglomeration characteristics in fluidised quartz bed combustion of phosphorus-rich biomass fuels, Energy Fuel 25 (2011) 937–947.

[44] J. Shabanian, P. Sauriol, N. Mostoufi, J. Chaouki, Performance evaluation of different approaches for early detection of defluidization, Powder Technol. 316 (2017) 139–147.

[45] F. Scala, Particle agglomeration during fluidised bed combustion: Mechanisms, early detection and possible countermeasures, Fuel Process. Technol. 171 (2018) 31–38.

[46] Y. Zhou, Q. Shi, Z. Huang, J. Wang, Y. Yang, Particle agglomeration and control of gas-solid fluidised bed reactor with liquid bridge and solid bridge coupling actions, Chem. Eng. J. 330 (2017) 840–851.

[47] L. Jia, R. Hughes, D. Lu, E.J. Anthony, I. Lau, Attrition of calcining limestones in circulating fluidized-bed systems, Ind. Eng. Chem. Res. 46 (15, 2007) 5199–5209.